JACS
JOURNAL OF THE AMERICAN CHEMICAL SOCIETY

Article

pubs.acs.org/JACS

Expanded Halogen-Bonded Anion Organic Networks with Star-Shaped Iodoethynyl-Substituted Molecules: From Corrugated 2D Hexagonal Lattices to Pyrite-Type 2-Fold Interpenetrated Cubic Lattices

Julien Lieffrig, Olivier Jeannin, and Marc Fourmigué*

Institut des Sciences Chimiques de Rennes, Université Rennes 1, UMR CNRS 6226, Campus de Beaulieu, 35042 Rennes, France

Supporting Information

ABSTRACT: Halogen bonding interactions between halide anions and neutral polyiodinated linkers are used for the elaboration of anion organic frameworks, by analogy with well-known MOF derivatives. The extended, 3-fold symmetry, 1,3,5-tris(iodoethynyl)-2,4,6-trifluorobenzene (**1**) cocrystallizes with a variety of halide salts, namely, $Et_3S^+I^-$, $Et_3MeN^+I^-$, $Et_4N^+Br^-$, $Et_3BuN^+Br^-$, Me-DABCO$^+I^-$, $Bu_3S^+I^-$, $Bu_4N^+Br^-$, $Ph_3S^+Br^-$, $Ph_4P^+Br^-$, and PPN$^+Br^-$. Salts with 1:1 stoichiometry formulated as (**1**)·(C^+,X^-) show recurrent formation of corrugated (6,3) networks, with the large cavities thus generated, filled either by the cations and solvent ($CHCl_3$) molecules and/or by interpenetration (up to 4-fold interpenetration). The 2:1 salt formulated as $(\mathbf{1})_2\cdot(Et_3BuN^+Br^-)$ crystallizes in the cubic $Ia\bar{3}$ space group (a = 22.573(5) Å, V = 11502(4) Å^3), with the Br^- ion located on $\bar{3}$ site and molecule **1** on a 3-fold axis. The 6-fold, unprecedented octahedral coordination of the bromide anion generates an hexagonal three-dimensional network of $Pa\bar{3}$ symmetry, as observed in the pyrite model structure, at variance with the usual, but lower-symmetry, rutile-type topology. In this complex system, the I centering gives rise to a 2-fold interpenetration of class Ia, while the cations and solvent molecules are found disordered within interconnected cavities. Another related cubic structure of comparable unit cell volume (space group $Pa\bar{3}$, a = 22.4310(15) Å, V = 11286.2(13) Å^3) is found with $(\mathbf{1})_2\cdot(Et_3S^+I^-)$.

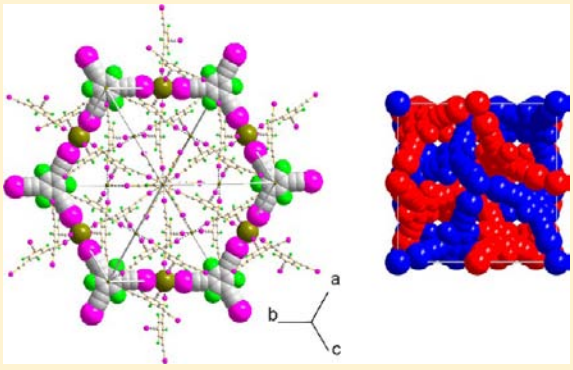

INTRODUCTION

Anion binding represents an important challenge, both from fundamental and applicative points of view.[1] This coordination chemistry of anions[2] is based on different noncovalent intermolecular interactions such as electrostatic interactions, coordination to metal ions,[3] anion−π interaction,[4] and most importantly hydrogen bonding. Recently, another interaction known as halogen bonding[5] was demonstrated to provide a highly efficient and directional interaction toward anion coordination.[6,7] Indeed, halogens in halocarbons exhibit a highly anisotropic electron distribution, with the existence of an electropositive region in the extension of the carbon−halogen bond, known as the σ-hole.[8] Its essentially electrostatic interaction[9] with Lewis bases give rise to a highly directional interaction, whose strength compares in some instances with the strongest hydrogen bonds.[10] Anions, and particularly the smallest halide ones, act as very good halogen bond acceptors,[6] as their negative charge is concentrated on one single atom. As a consequence, they lead to extremely short C−Hal···X^- distances. The strongest interactions are found with the heaviest halogens with Hal = I > Br ≫ Cl ≫ F, while strong interactions are reported with every X^- halide anion. Because of their spherical nature, halide anions as halogen bond acceptors can adopt a variety of coordination numbers, with up to eight halogen bonds and acute C−Hal···X^-···Hal−C angles (down to 60°).[6] On the basis of this interaction, numerous extended anionic networks were described, from the cocrystallization of naked halide anion (i.e., with noncoordinating cations) together with polydentate halogen bond donors[11] such as diiodoacetylene,[12] 1,4-diiodotetrafluorobenzene,[13] 1,4-bis(iodoethynyl)benzene,[14] tetraiodoethylene[15] or tetrabromomethane[16] (Scheme 1). By analogy with well-known MOF derivatives where metal cations form the nodes of extended architectures,[17,18] the combination of halides as nodes and polyiodinated molecules as linkers can therefore be used for the elaboration of anion organic frameworks. Depending on the number of iodine atoms in the neutral halogen bond donor, the nature and size of the cationic counterion, the dimensionality of the resulting networks can be engineered, and numerous 1D and 2D structures[6] have been described but only a few 3D architectures, essentially adamantanoid ones[16] based on the combination of tetrahedral CBr_4 with chloride or iodide anions.

Received: January 22, 2013
Published: March 26, 2013

   dx.doi.org/10.1021/ja400740v | *J. Am. Chem. Soc.* 2013, 135, 6200−6210

Scheme 1. Examples of Di-, Tri-, and Tetratopic Neutral Molecules Acting as Halogen Bond Donor toward Halide Anions

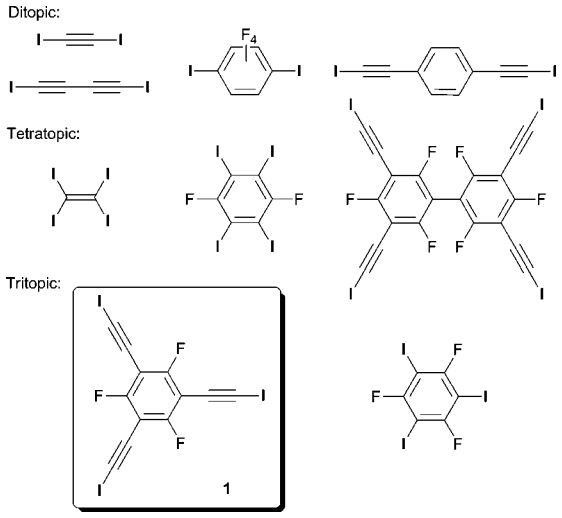

These strategies were also particularly developed by Kato and Yamamoto for the elaboration of conducting, tetrathiafulvalene-based (TTF) cation radical salts where the anionic counterpart consists into such layered halogen-bonded networks.[19] Association of different halide anions and/or different neutral ditopic and tetratopic halogenated molecules afforded striking 2D or 3D structures where the anions form insulating tubular sheaths around the stacks of oxidized TTF molecules.[20] Attempts to increase the size of tetratopic neutral molecules led to 3D networks with PtS-type structures with 8-fold interpenetration.[21] By comparison, *tritopic* neutral halogenated molecules were much less investigated, while they potentially offer very attractive features for the elaboration of 3-fold symmetry structures like 2D honeycomb or 3D cubic ones. Actually, the tridentate halogen bond donor 1,3,5-triiodo-2,4,6-trifluorobenzene (Scheme 1) was already shown to recurrently afford 2D (6,3) networks upon cocrystallization with halide salts of various counterions, the smallest ones (Et_4N^+, Et_4P^+) being able to stabilize the perfect honeycomb networks,[22] while larger cations (nBu_4N^+, PPh_4^+) afforded strongly corrugated (6,3) networks.[23] In order to favor the formation of larger 2D or 3D cavities, which could accommodate larger cations and also eventually cation radicals such as $TTF^{+\bullet}$, we designed an extended analogue of 1,3,5-triiodo-2,4,6-trifluorobenzene, by replacing the three iodine atoms by iodoethynyl moieties, to give the 1,3,5-tris(iodoethynyl)-2,4,6-trifluorobenzene **1**. Its cocrystallization was then undertaken with a variety of organic cations, from the smallest triethylsulfonium (Et_3S^+) to the larger bis(triphenylphosphoranylidene)ammonium ($Ph_3P{=}N^+{=}PPh_3$, PPN), revealing a cornucopia of structural motifs, from more or less corrugated 2D honeycomb lattices to 2-fold interpenetrated, pyrite-type, cubic lattices, with an unprecedented octahedral coordination around the halide anion.

RESULTS AND DISCUSSION

Syntheses and Solid State Structures of 1,3,5-Trifluoro-2,4,6-tris(iodoethynyl)benzene 1. Molecule **1** was prepared (Scheme 2) by analogy with similar iodoethynyl derivatives in two steps,[24] first a Sonogashira coupling of 1,3,5-trifluoro-2,4,6-triiodo-benzene with trimethylsilylacetylene in

Scheme 2. Synthetic Procedure to 1[a]

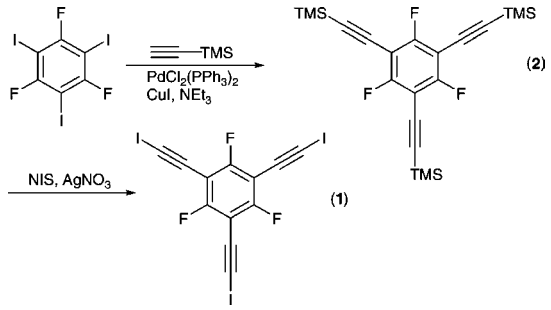

[a]NIS stands for *N*-iodosuccinimide.

the presence of $PdCl_2(PPh_3)_2$ and CuI to afford **2** in 54% yield, followed by reaction of **2** with *N*-iodosuccinimide and $AgNO_3$ to give the title compound **1** in 59% yield. Recrystallization from hexane/CH_2Cl_2 1:1 afforded **1** as single crystals, while a 1:1 DMSO solvate was isolated from DMSO-d_6.

The molecular structures of the three compounds **1**, **2**, and **1**·DMSO were determined from single crystal X-ray diffraction. **1** crystallizes in the triclinic system, space group $P\bar{1}$, with one molecule in general position in the unit cell. Molecules organize into layers (Figure 1), held together by I···I halogen bonds,

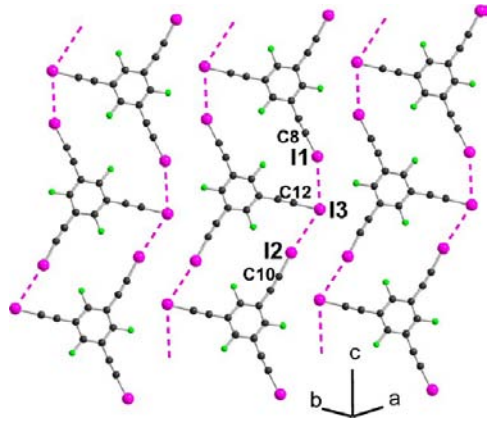

Figure 1. Projection view of one layer formed by molecules **1** in the solid state, with dotted lines for I···I distances shorter than 4 Å, with following geometrical characteristics. I(1)···I(3): 3.937(4) Å and C(8)–I(1)···I(3): 155.6(1°) and I(1)···I(3)–C(12): 73.7(1)°; I(2)···I(3): 3.945(8) Å, C(10)–I(2)···I(3): 164.7(1)° and I(2)···I(3)–C(12): 70.5(1)°.

with atoms I(1) and I(2) acting as halogen bond donors toward I(3), which acts as halogen bond acceptor.

1·DMSO crystallizes in the orthorhombic system, space group *Pnma* with molecule **1** and DMSO lying flat on the mirror plane (Figure 2). Iodine atoms I(1) and I(3) act as halogen bond donors toward the DMSO oxygen atom, while iodine atom I(2) direct toward I(1). The two I···O halogen bonds are particularly short when compared with other reported halogen bonded DMSO with perfluorinated iodobenzene derivatives,[25] as the reduction ratio, defined as $rr = d_{I\cdots O}/(R_{vdW}(I) + R_{vdW}(O))$ takes a 0.77–0.78 value, demonstrating once again the strong halogen bond donor character of iodoacetylene derivatives. Note also the strong directionality, with C–I···O angles close to 180° and I···O–S angles close to 120°.

dx.doi.org/10.1021/ja400740v | J. Am. Chem. Soc. 2013, 135, 6200–6210

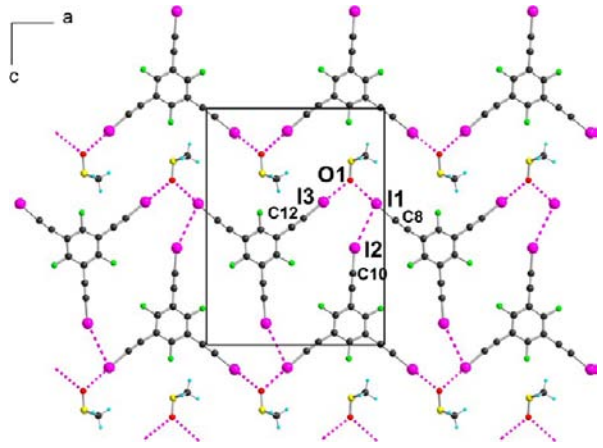

Figure 2. Projection view along the *b* axis of one layer of **1**·DMSO. Halogen bonds are marked with dotted purple lines, with following geometrical characteristics. I(1)···O(1): 2.755(4) Å, C(8)–I(1)···O(1): 179.2(2)°; I(3)···O(1): 2.714(4) Å, C(12)–I(3)···O(1): 179.2(2)°; I(2)···I(1): 3.894(1), C(10)–I(2)···I(1): 158.2(2)°.

The synthetic TMS intermediate **2** crystallizes in the trigonal system, space group *P*31*c*, with molecule **2** located on the 3-fold axis (Figure 3). The molecules organize into closed-packed

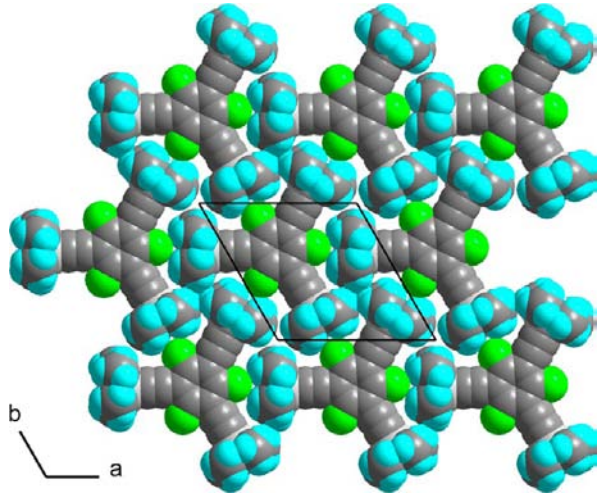

Figure 3. Projection view along the *c*-axis of one layer in **2**.

layers along the *c*-axis, with the methyl groups pointing toward the fluorine atoms of neighboring molecules.

The cocrystallization of **1** with various halide salts (Scheme 3) has been undertaken with the hope to stabilize (6,3) networks where the cation would fit within the hexagonal cavity formed by molecules **1**, halogen bonded to the halide anion. We will see in the following that a variety of structural motifs have been actually obtained, depending on the size and shape of each cation. Two groups of structures stand out, those with a 1:1 stoichiometry, formulated as (**1**)·(C^+,X^-), and those with a 2:1 stoichiometry, (**1**)$_2$·(C^+,X^-), with two iodinated molecules for one salt. They will be detailed below successively, starting with the smallest cations. Note that with Et_3S^+,I^- and Bu_4N^+,Br^- salts, two adducts were obtained with respectively 1:1 and 2:1 stoichiometry, depending on the experimental conditions. They will be described in the two different sections.

Scheme 3. Halide Salts Investigated in Cocrystallization Experiments with 1

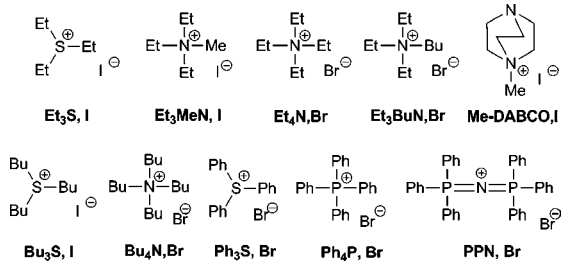

Halide Adducts of 1:1 Stoichiometry. Seven examples of 1:1 adducts were isolated. The smallest investigated cation is the triethylsulfonium, as iodide salt. It crystallizes with **1** and chloroform molecules in the monoclinic system, space group $P2_1/n$, with neutral molecule **1**, the salt and one $CHCl_3$ molecule in general position in the unit cell. As shown in Figure 4, the iodide anion is halogen bonded to three iodine

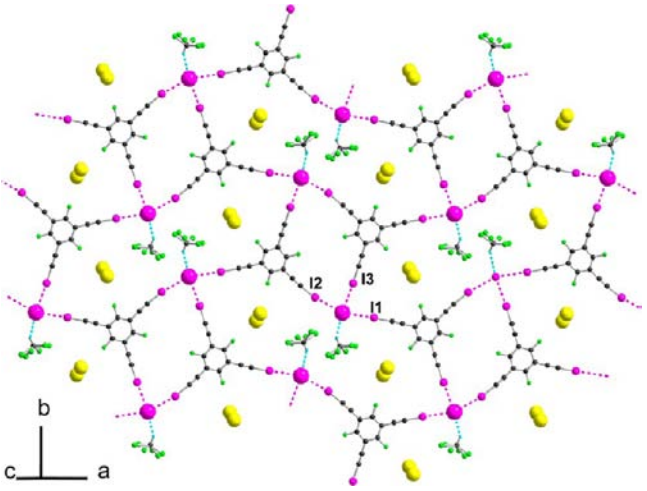

Figure 4. Projection view of the anionic layer in (**1**)·(Et_3S,I)·$CHCl_3$. Only the two disordered sulfur atoms of the Et_3S^+ cations are represented as yellow spheres. Halogen bonds are drawn as pink lines, C–H hydrogen bonds as blue dotted lines.

atoms of three different molecules **1** with short I···I distances (Table 1), as already observed with the smaller 1,3,5-trifluoro-2,4,6-triiodobenzene,[22,23] but with an added hydrogen bond with a $CHCl_3$ molecule, affording a distorted square planar coordination, rather than the trigonal coordination stabilizing the (6,3) honeycomb network. The resulting complex anionic network generates a cavity accommodating the $CHCl_3$ molecule, with the Et_3S^+ cation disordered on two positions.

With larger cations, (6,3) networks with 3-fold coordinated halide anions were recurrently identified, with however different geometries related to (i) the planarity of the network and (ii) its possible interpenetration. Indeed, within (**1**)(Et_4N,Br)·$CHCl_3$ and (**1**)(Bu_4N,Br), the sum of the three I···I^-···I angles, noted Σ_{IXI} in Table 1, amounts respectively to 289 and 286°, indicating a strong distortion from planar coordination. As shown in Figure 5, the (6,3) networks are then strongly corrugated and pile up on top of each other, leaving cavities for the embedded cations. Such a motif was already observed for example in similar adducts with 1,3,5-trifluoro-2,4,6-triiodobenzene,[23] when the size of the cation and that of the hexagonal hole are not adapted to each other.

dx.doi.org/10.1021/ja400740v | *J. Am. Chem. Soc.* 2013, 135, 6200–6210

Table 1. Geometrical Features of the Halogen Bond Interactions in the Different 1:1 Salts[a]

compound	X^-	coord no.[b]	I···X^- dist (Å)		*rr*	C–I···X^- ang (°)	Σ_{IXI}
(**1**)(Et_3S,I)·S	I^-	3	I(1)	3.510(1)	0.85	175.0(2)	319.4
			I(2)	3.437(1)	0.83	170.8(2)	
			I(3)	3.436(1)	0.83	177.7(2)	
(**1**)(Et_3MeN,I)·S	I^-	3	I(1)	3.427(2)	0.83	175.2(3)	337.0
			I(2)	3.450(2)	0.83	177.1(3)	
			I(3)	3.477(2)	0.84	174.1(3)	
(**1**)(Et_4N,Br)·S	Br^-	3	I(1)	3.349(1)	0.85	171.0(2)	289.3
			I(2)	3.251(2)	0.83	178.2(2)	
			I(3)	3.282(2)	0.83	176.7(2)	
(**1**)(Me-DABCO,I)· S	I^-	3	I(1)	3.382(1)	0.82	173.5(2)	351.8
			I(2)	3.462(1)	0.84	176.5(2)	
			I(3)	3.592(1)	0.87	161.1(2)	
(**1**)(Bu_3S,I)	I^-	3	I(1)	3.386(1)	0.82	166.5(1)	351.3
			I(2)	3.399(1)	0.82	167.8(1)	
			I(3)	3.433(1)	0.83	173.2(1)	
(**1**)(Bu_4N,Br)	Br^-	3	I(1)	3.214(2)	0.82	167.7(2)	246.4
			I(2)	3.248(2)	0.83	176.7(3)	
			I(3)	3.186(1)	0.81	173.3(2)	
(**1**)(PPN,Cl)	Cl^-	3	I(1)	3.050(2)	0.80	175.5(1)	353.5
			I(2)	3.081(2)	0.81	173.8(1)	
			I(3)	3.054(2)	0.80	170.8(1)	

[a]The reduction ratio (*rr*) is calculated relative to the cut-off values of 3.79, 3.93, and 4.14 Å for the C–I···Cl^-, C–I···Br^- and C–I···I^- contacts, respectively (see text). S stands for $CHCl_3$ molecule, and Σ_{IXI} represents the sum of the three I···X^-···I angles around the halide atoms. [b]The number of iodine atoms by which the anion is coordinated.

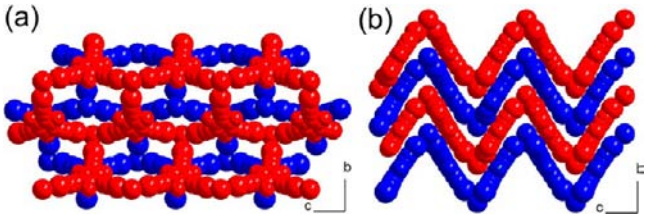

Figure 5. Views of the corrugated (6,3) networks observed in (a) (**1**)(Et_4N,Br)·$CHCl_3$ and (b) (**1**)(Bu_4N,Br). The cations and solvent molecules are not represented.

At variance with the two previous salts, those obtained with the *N*-methyl-diazabicyclooctane iodide, (Me-DABCO,I), and with the even larger PPN cation, afforded almost planar (6,3) networks, with Σ_{IXI} values of 352–353°, allowing for a perfect fit of the cations, together with extra $CHCl_3$ molecules, within the hexagonal cavities delineated by the stacking of two layers of neutral molecules **1**, rotated by 60°. As shown in Figure 6a for (**1**)(Me-DABCO,I)·$CHCl_3$, the added hydrogen bond of the chloroform to the iodide distorts the trigonal coordination around the iodide, while in (**1**)(PPN,Cl)·$(CHCl_3)_4$, the solvent molecules are disordered and the chloride coordination is perfectly trigonal.

The former examples demonstrate that the cavities generated by the expanded molecule **1** are often too large to accommodate the cations, leading to strongly corrugated (6,3) layers and/or solvent inclusion. This constraint can be also circumvented by interpenetration, a rare situation among halogen bonded systems,[26,27] as illustrated here in the two last examples of 1:1 adducts with Bu_3SI and Et_3MeNI. Indeed, as shown in Figure 7, each iodide anion in (**1**)(Bu_3S,I) is coordinated by three iodine of three different molecules **1**, leading to the formation of 2-fold interpenetrated (6,3) networks.

An even more complex structure is found with the triethylmethylammonium iodide salt, (**1**)·(Et_3MeN,I)·$CHCl_3$. The sum of the three I···I^-···I angles, noted Σ_{IXI} in Table 1, amounts to 337°, indicating a distortion from planar coordination. This 3-fold coordination around the iodide ion does not lead to the anticipated (6,3) two-dimensional network, since one of the

Table 2. Geometrical Features of the Halogen Bond Interactions in the 2:1 Salts $(1)_2(Bu_4N,Br)$ and $(1)_2(Ph_3S,Br)$[a]

compound	X^-	coord no.[b]	I···X^- dist (Å)		*rr*	C–I···X^- ang (°)
$(1)_2(Bu_4N,Br)$	Br^-	4	I(1)	3.269(1)	0.83	163.3(2)
			I(2)	3.331(1)	0.85	173.6(2)
			I(3)	–	–	–
$(1)_2(Ph_3S,Br)$	Br^-	4	I(1)	3.335(2)	0.85	168.60(9)
			I(2)	3.198(2)	0.81	177.24(9)
			I(3)	–	–	–
$(1)_2(Et_3BuN,Br)$	Br^-	6	I(1)	3.249(7)	0.83	175.1(4)
$(1)_2(Et_3S,I)$	I^- [c]	6	I(1)	3.218(1)	0.78	172.4(3)
			I(1)	3.172(1)	0.77	176.5(4)

[a]The reduction ratio (*rr*) is calculated relative to the cut-off values of 3.93 and 4.14 Å for the C–I···Br^- and C–I···I^- contacts, respectively (see also Table 1). [b]The number of neutral molecules by which the anion is coordinated. [c]Iodide anion with 0.5 occupancy.

dx.doi.org/10.1021/ja400740v | *J. Am. Chem. Soc.* 2013, 135, 6200–6210

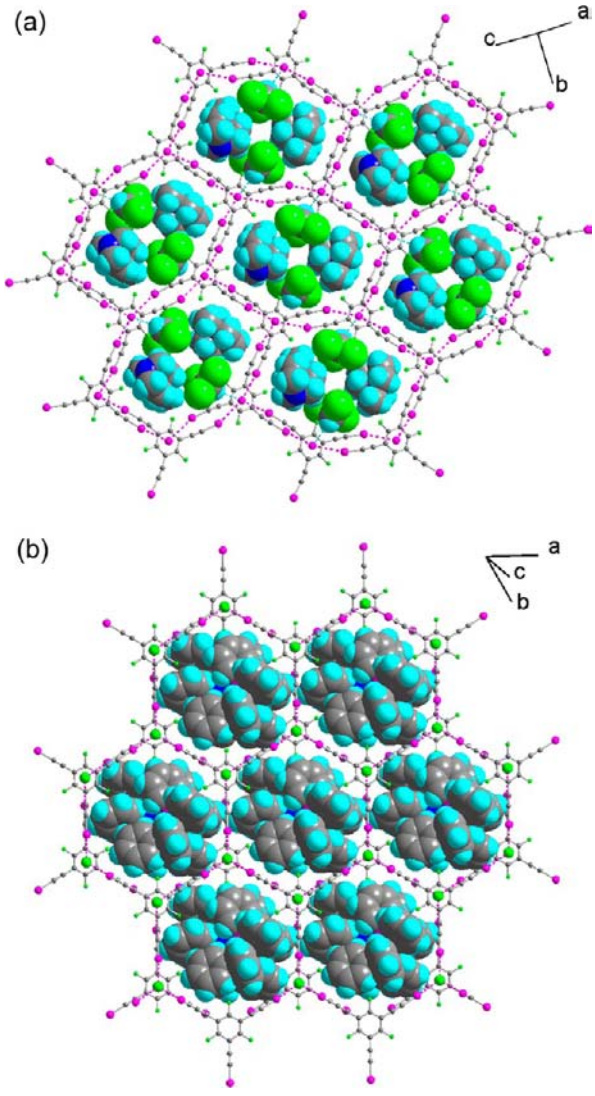

Figure 6. (a) View of the planar (6,3) network in (**1**)(Me-DABCO,I)·$CHCl_3$. The I···I^-contacts are shown with purple dotted lines and the H···I^- contacts with cyan dotted lines. (b) View of the planar (6,3) network in (**1**)(PPN,Cl)·$(CHCl_3)_4$. The $CHCl_3$ molecules are omitted for clarity, and the I···Cl^-contacts are shown with purple dotted lines.

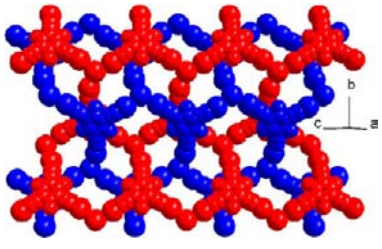

Figure 7. The two interpenetrated halogen bonded networks in (**1**)(Bu_3S,I). The Bu_3S^+ cations are not represented.

three molecules is rotated out of this plane (Figure 8a), but generates a complex three-dimensional anionic network with large, 14 Å wide, cavities. The symmetry elements of the $P2_1/c$ space group generate a 4-fold interpenetration (class IIIa),[28] twice by translation and twice by inversion (Figure 8b).

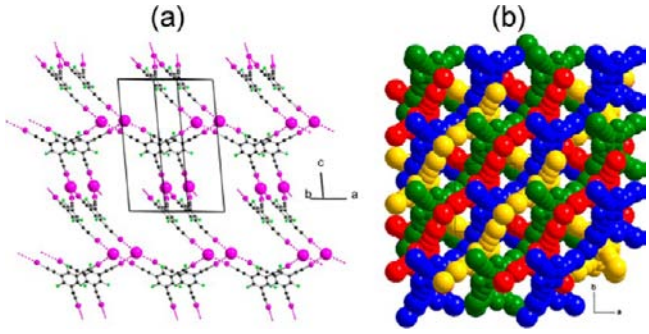

Figure 8. (a) One of the four halogen bonded sublattices in (**1**)(Et_3MeNI)·$CHCl_3$. (b) View of the 4-fold interpenetrated halogen-bonded network in (**1**)(Et_3MeN, I)·$CHCl_3$. The Et_3MeN^+ cation and $CHCl_3$ molecules have been omitted for clarity.

As preliminary conclusions for these series of 1:1 salts, it appears that the 3-fold symmetry of molecule **1** favors in many instances a 3-fold coordination of the halide anion, affording systematically the anticipated (6,3) networks. A fully planar honeycomb network is only obtained with the largest PPN cation, with two cations to fill the large hexagonal cavity, while the other much smaller cations circumvent this size problem by either a strong corrugation of the (6,3) network, and/or by interpenetration of two sublattices as observed with Bu_3SI, or even four sublattices with the smaller Et_3MeN^+ cation. Similar adaptations were observed earlier with the smaller 1,3,5-trifluoro-2,4,6-triiodobenzene (See Scheme 1), which affords regular, planar (6,3) networks with small cations fitting perfectly within the cavity,[22] while larger ones lead to severe distortions from planarity.[23] By comparison, the much larger cavities generated from **1** allow here for another possibility, interpenetration, as beautifully illustrated in the salts with Bu_3S^+,I^- (Figure 7) and Et_3MeN^+,I^- (Figure 8).

In some instances, we were able to isolate cocrystals incorporating two neutral molecules for one salt, leading to a 4-fold or 6-fold coordination around the halide anion, as described below. While monoclinic structures with a 4-fold coordination around the bromide anion were found with the *n*-Bu_4N^+ and Ph_3S^+ cations, remarkable cubic structure with a 6-fold coordination around the halide anion were identified with the $Et_3BuN^+Br^-$ and $Et_3S^+I^-$ salts.

Halide Adducts with Two Iodinated Molecules. The salt $(\mathbf{1})_2(Bu_4N,Br)$ crystallizes in the monoclinic system, space group $C2/c$, with molecule **1** in general position, while both *n*-Bu_4N^+ cation and Br^- anion are located on the 2-fold axis, hence the 2:1 stoichiometry. Each bromide anion is now coordinated by four iodine atoms in a distorted tetrahedral environment, leaving one free iodine atom in molecule **1** (Figure 9a). Geometrical characteristics of these short halogen contacts are collected in Table 2 for these 2:1 salts. This coordination pattern leads to the formation of ribbons running along $2a+c$. A similar 4-fold coordination is identified in the $Ph_3S^+Br^-$ salt, which crystallizes in the monoclinic system, space group $C2/c$ with molecule **1** in general position and both Ph_3S^+ cation (disordered on two positions) and Br^- anion on the 2-fold axis (Figure 9b).

As mentioned above, the Et_3BuN^+, Br salt afforded upon cocrystallization with **1** a cubic structure formulated as $(\mathbf{1})_2(Et_3BuN,Br)$, which crystallizes in the centrosymmetric $Ia\bar{3}$ space group [a = 22.573(5) Å, V = 11502(4) Å^3], with the Br^- ion located on $\bar{3}$ site and molecule **1** on a 3-fold axis

dx.doi.org/10.1021/ja400740v | J. Am. Chem. Soc. 2013, 135, 6200−6210

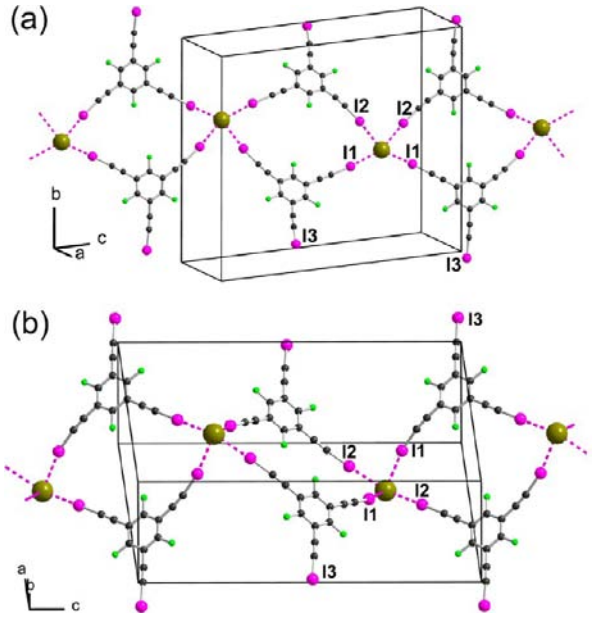

Figure 9. (a) View of a halogen bonded ribbon running along (2a+c) in $(\mathbf{1})_2(Bu_4N,Br)$. The Bu_4N^+ cations have been omitted for clarity. (b) View of a halogen bonded ribbon running along (c) in $(\mathbf{1})_2(Ph_3S,Br)$. The Ph_3S^+ cations have been omitted for clarity.

(Figure 10). The Et_3BuN^+ cation could not be properly identified in the Fourier difference maps, indicating a strong disorder, attributable to its unsymmetrical character (see below). At variance with the two previous 2:1 salts, all three iodine atoms of molecule **1** are now engaged in halogen bonding interaction with the halide anion, located by symmetry at the center of a perfect octahedron (Figure 10a).

This combination of triangular nodes (provided by molecule **1**) with octahedral nodes (around the halogen-bonded anion) generates a three-dimensional solid state organization illustrated in Figure 10b. This underlying framework (Figure 10c) has symmetry $Pa\bar{3}$, while the *I* centering generates two interpenetrating frameworks, with $Ia\bar{3}$ symmetry for the whole crystal. Yaghi et al. related this specific connectivity between triangular and octahedral nodes within one single $Pa\bar{3}$ framework to the pyrite-type structure, if ignoring the S−S bond in pyrite-type FeS_2.[29] This topology is rather rare, as the interaction of triangular and octahedral nodes usually leads to the lower-symmetry rutile-type topology.[30,31] It has been identified only in a few instances in metal organic frameworks (MOF), where triangular ligands, anionic or neutral, coordinate metallic centers (Cd^{2+}, Zn_4O^{6+}) ions in an octahedral way.[29,32]

From this analogy with the pyrite structure, we can determine the *u* parameter, which in FeS_2 gives the position of the S atom along the ⟨111⟩ axes (Figure 11). Indeed, in the higher symmetry fluorite (CaF_2) structure, the F^- ions are located on the center positions of the eight subcubes of the cubic unit cell at (1/4 1/4 1/4) and symmetry-equivalent positions. The pairing of the two S atoms into a S_2^{2-} unit in pyrite moves them from this position ($u = 0.25$) to a *u* value of 0.385 (Figure 11a).[33] In the cubic $(\mathbf{1})_2(Et_3BuN,Br)$ salt, each neutral molecule **1** is coordinated to three bromide ions (Figure 11b), in the same way the sulfur atoms in pyrite are coordinated to three Fe^{II} ions. Considering one of the two interpenetrated networks (Figure 11b) places the centroïd of one neutral

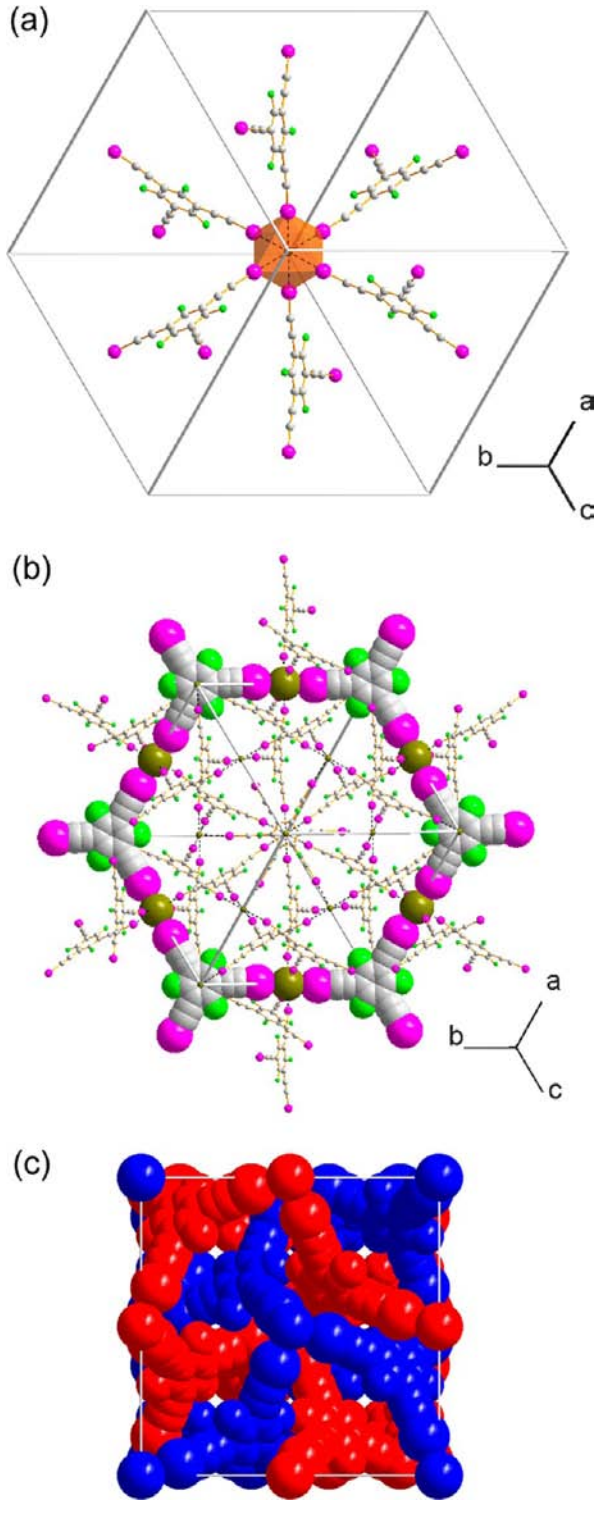

Figure 10. Views of the unit cell of $(\mathbf{1})_2(Et_3BuN,Br)$ with (a) the octahedral coordination around the bromide ion, (b) a projection view along the (111) axis, and (c) the two interpenetrated networks.

molecule **1** at $u = 0.355$ (Figure 11b,c), a value close to that observed in pyrite itself.

This structure is one of the very rare examples of interpenetrated structures where the nodes are built out of relatively weak halogen bonding interactions,[26,27] by comparison with analogous MOF structures where a much stronger metal coordination generates the octahedral nodes. Despite this

dx.doi.org/10.1021/ja400740v | J. Am. Chem. Soc. 2013, 135, 6200−6210

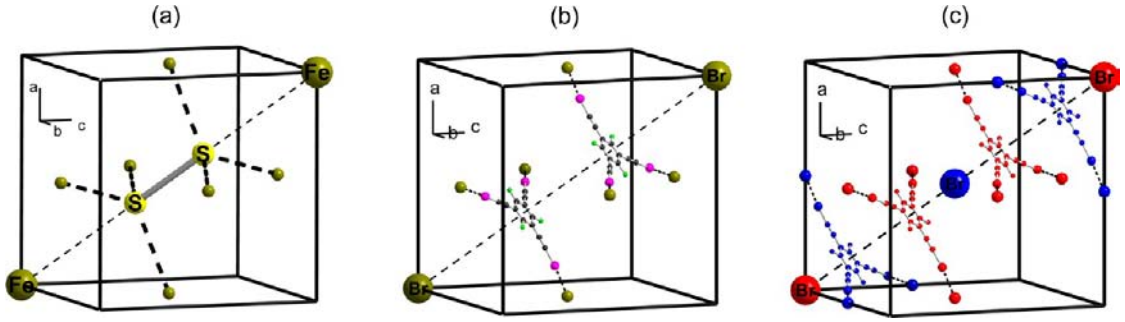

Figure 11. (a) Detail of the structure of pyrite FeS_2 with the S_2^{2-} anion linked to 6 equivalent Fe^{2+} cations. (b) The same view for the structure of $(\mathbf{1})_2(Et_3BuN,Br)$, showing only molecules and ions contributing to one of the two interpenetrated networks. (c) The same view for the structure of $(\mathbf{1})_2(Et_3BuN,Br)$, showing molecules contributing to both sublattices (in red and blue), thanks to *I* centering.

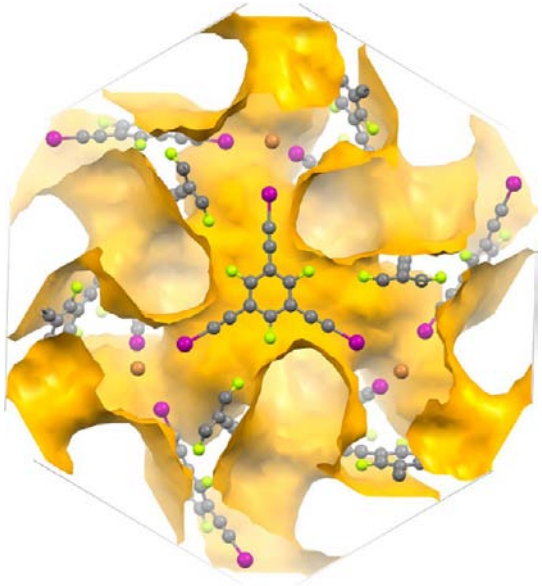

Figure 12. Projection view of the unit cell of $(\mathbf{1})_2(Et_3BuN,Br)$ along the (111) axis, highlighting the interconnected cavities filled by cations and solvent molecules (not shown).

double interpenetration, the structure still presents interconnected cavities (Figure 12), occupied by the disordered Et_3BuN^+ cations and most probably a large number of $CHCl_3$ molecules. Indeed, the calculated free volume amounts to 6250 Å^3, while the volume occupied by the eight Et_3BuN^+ cations should not exceed ≈2400 Å^3. These solvent molecules are easily lost when the crystals are taken out of the mother liquor, leading to a rapid amorphization of the crystals.

This 2-fold interpenetrated cubic structure with its interconnected cavities is also reminiscent of the bicontinuous cubic phases frequently observed in lyotropic[34] or thermotropic[35] liquid crystals, where the fluid phase (solvent or melted alkyl chains) would be replaced here by the cation/solvent mixture. Furthermore, in these systems, epitaxial relationship for the hexagonal-to-cubic phase transition have been identified,[36] both in soft matter[37] as in mesoporous materials,[38] illustrating the structural relationship between the hexagonal motifs observed in the 1:1 salts and the cubic phase found in this 2:1 phase with Et_3BuNBr salt. As reported by Ward and Horner,[39] this analogy between high symmetry molecular crystalline structures and soft matter hexagonal or cubic microstructures might find its origin in (i) predestined topologies of molecular components, (ii) conformational softness that permits curvature at small length scales, and (iii) aggregation to increase this length scale and stabilize curved surfaces needed for high symmetry lattices. The system described here in $(\mathbf{1})_2(Et_3BuN,Br)$ combines indeed these three characters, that is, (i) a rigid, 3-fold symmetry, molecular component **1**, (ii) a disordered asymmetrical cation bringing softness, and (iii) halogen bonding as the strong and efficient aggregation tool for the generation of higher length scale motifs. The robustness of this cubic phase is also illustrated by the last 2:1 stoichiometry structure described here, obtained with Et_3S^+,I^- and formulated as $(\mathbf{1})_2(Et_3S,I)$.

$(\mathbf{1})_2(Et_3S,I)$ crystallizes indeed in the cubic system, space group $Pa\bar{3}$ with a unit cell volume, V = 11286.2(13) Å^3, comparable to that described above with Et_3BuNBr. The loss of *I* centering thus leads to two crystallographically independent molecules **1**, each on a 3-fold axis, together with one Et_3S^+ cation, with 1/3 occupation parameter, disordered on six positions around an iodide ion located on a $\bar{3}$ site, while a second iodide ion, with 1/2 occupancy, sits on the 3-fold axis and is halogen bonded in an octahedral way to two crystallographically independent **1** molecules (Figure 13). As a consequence of this 1/2 occupancy, the $I\cdots I^-$ distances to the iodide anion are actually much shorter (Table 2) than in the other examples involving such $I\cdots I^-$ contacts (See Table 1). As shown in Figure 13, this structure is closely related to that of $(\mathbf{1})_2(Et_3BuN,Br)$ described above (Figure 12). The main differences are (i) the differentiation between two kinds of iodide ions, either within the octahedral halogen bonded motif with 1/2 occupancy or free and surrounded by the disordered Et_3S^+ cations and (ii) the proper localization of the cationic counterpart, which occupies, in the $Pa\bar{3}$ space group, four sites among the eight equivalent sites available for cation and solvent in the $Ia\bar{3}$ structure of the Et_3BuNBr salt. As a consequence of the localization of the Et_3S^+ cation in the structure, the interconnected voids, which in $(\mathbf{1})_2(Et_3BuN,Br)$ were occupied by disordered cations and solvent molecules (Figure 13), are essentially filled, leaving only much smaller unconnected cavities shown in Figure 14, which now represent 16.4% of the unit cell volume, filled only with solvent molecules.

■ CONCLUSIONS

While the smaller triiodotrifluorobenzene molecule had been shown to afford (6,3) honeycomb-like networks upon cocrystallization with halide salts, accommodating rather small cations, the extended, star-shaped iodoethynyl-substituted molecule **1** demonstrated an exceptional ability to cope with a variety of supramolecular solid state organizations, depending

dx.doi.org/10.1021/ja400740v | *J. Am. Chem. Soc.* 2013, 135, 6200−6210

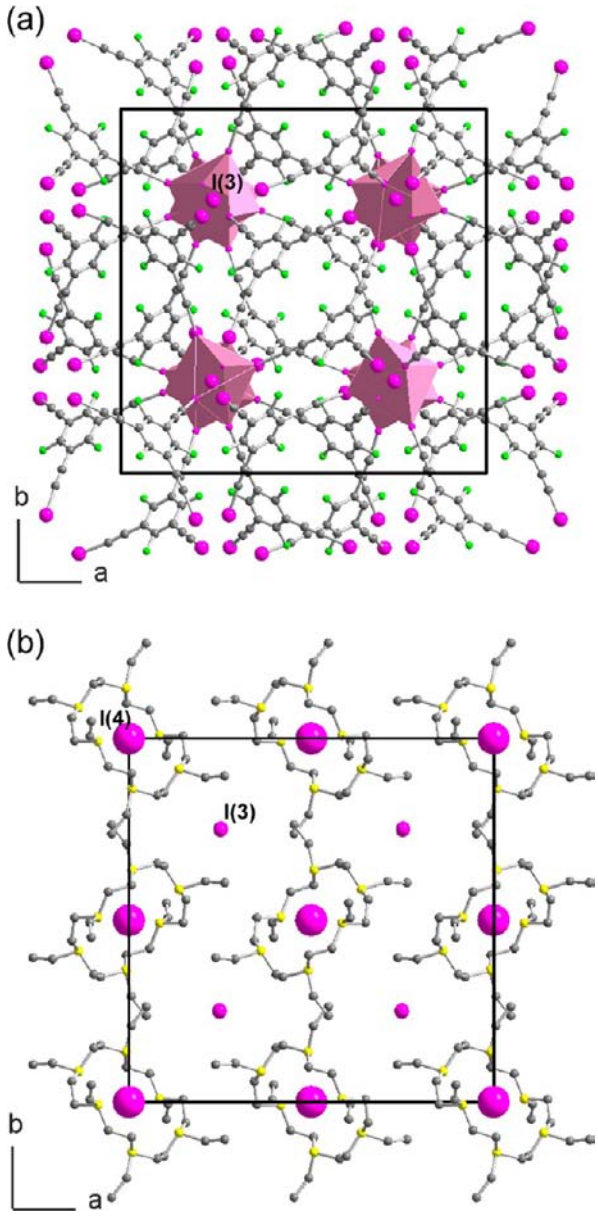

Figure 13. Projection views along c of the unit cell of $(\mathbf{1})_2(Et_3S,I)$ showing selectively (a) molecules **1** engaged in the octahedral coordination of the I^- ion, labeled I(3) and located on 3-fold axis, and (b) Et_3S^+ cations disordered on six positions around the iodide ion labeled I(4) (with larger radius) located on a $\bar{3}$ site. The superposition of the two figures gives the full projection view.

on the cation size as well as on the **1**/salt ratio. The potentially porous structures generated by the halogen bonding interactions between the rigid molecule **1** and the halide anions stabilize through interpenetration (up to 4-fold interpenetration with Et_3MeN^+,I^-) in the 1:1 adducts, providing also, with 2:1 stoichiometry, the first example, to our knowledge, of a halogen-bonded cubic-type structure where the halide anion is 6-fold coordinated in a perfect octahedron, as a mirror image of the usual octahedral coordination of metal cations. Indeed, as mentioned above in the Introduction, because of their spherical nature, halide anions can adopt a variety of coordination numbers, with up to eight halogen bonds and acute C−Hal···X^-···Hal−C angles (down to 60°).[6] We have found here an illustration of this versatility, with coordination numbers of three, four and six.

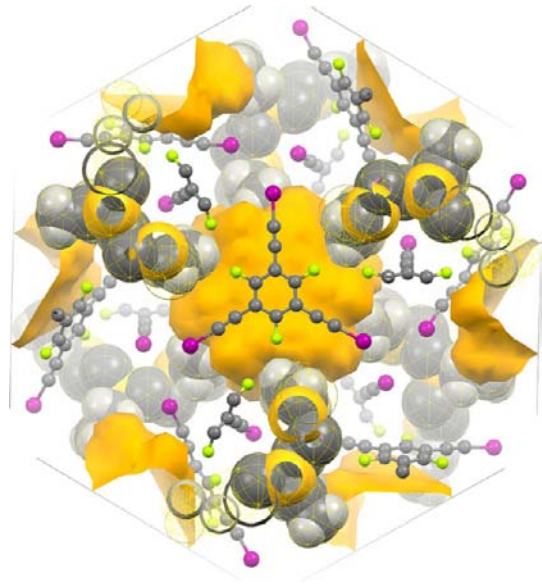

Figure 14. Projection view of the unit cell of $(\mathbf{1})_2(Et_3S,I)$ along the (111) axis, highlighting the unconnected cavities (with yellow outer surface). Compare also with Figure 12.

Table 3. Experimental Conditions for the Crystallization of the Ternary Salts

salt	salt quantity	**1** quantity	product
Et_3S,I	8.9 mg, 36.2 μmol	20.0 mg, 34.4 μmol	$(\mathbf{1})(Et_3S,I)\cdot CHCl_3$
Et_3MeN,I	4.2 mg, 17.2 μmol	10.0 mg, 17.2 μmol	$(\mathbf{1})(Et_3MeN,I)\cdot CHCl_3$
DABCO, I	4.4 mg, 17.3 μmol	10.0 mg, 17.2 μmol	$(\mathbf{1})(DABCO,I)\cdot CHCl_3$
Et_4N,Br	15.4 mg, 50.0 μmol	12.4 mg, 21.3 μmol	$(\mathbf{1})(Et_4N,Br)\cdot CHCl_3$
Bu_3S,I	5.7 mg, 17.3 μmol	10.0 mg, 17.2 μmol	$(\mathbf{1})(Bu_3S,I)$
Et_3BuN,Br^a	12.6 mg, 52.9 μmol	48.0 mg, 82.5 μmol	$(\mathbf{1})_2(Et_3BuN)Br$
Bu_4N,Br	15.4 mg, 47.8 μmol	22.0 mg, 37.8 μmol	$(\mathbf{1})(Bu_4N,Br)$
Bu_4N,Br	5.5 mg, 17.1 μmol	10.0 mg, 17.2 μmol	$(\mathbf{1})_2(Bu_4N,Br)$
PPN,Cl	7.2 mg, 17.2 μmol	10.0 mg, 17.2 μmol	$(\mathbf{1})(PPN,Cl)$
Ph_3S,Br	5.9 mg, 17.2 μmol	10.0 mg, 17.2 μmol	$(\mathbf{1})_2(SPh_3,Br)$

[a]Experiment performed in 1,1,2-trichloroethane.

While the two first coordination patterns are not exceptional,[6] six-coordinated halide anions have been described in a few instances,[19a,20] and only with a trigonal prismatic (D_{3h}) geometry. The unprecedented octahedral geometry around the halide anion is furthermore associated with a compression effect. Indeed, it has been pointed out that larger coordination numbers around halide anions were associated with longer halogen bond distances, as the first halogen bonds deactivate the Lewis base character of the halide toward a larger number of interactions, with also possible steric interactions between iodine atoms. We note in the various salts described here that the averaged I···Br^- distances increase indeed from 3.249 Å in the 3-fold coordinated systems to the longer 3.282 Å in the 4-fold coordinated systems, while it counterintuitively decreases back to 3.249 Å in the octahedral geometry. Furthermore, in this cubic $(\mathbf{1})_2(Et_3BuN,Br)$ salt, and considering one of the two interpenetrated networks of $Pa\bar{3}$ symmetry, the structural analogy with pyrite-type structures places the centroïd of neutral molecule **1** at u = 0.355, a value close to that observed in pyrite itself (u = 0.385). The robustness of this cubic structure is further illustrated by the 2:1 salt with $Et_3S^+I^-$ where the size and symmetry adaptation of the cation allows for its

dx.doi.org/10.1021/ja400740v | J. Am. Chem. Soc. 2013, 135, 6200−6210

Table 4. Crystallographic Data (S in Compounds' Names Stands for $CHCl_3$)[a]

compound	2	1	1·DMSO	(1)(Et_3S,I)·S	(1)(Et_3MeN,I)·S
Formula	$C_{21}H_{27}F_3Si_3$	$C_{12}F_3I_3$	$C_{14}H_6F_3I_3OS$	$C_{19}H_{16}Cl_3F_3I_4S$	$C_{20}H_{19}Cl_3F_3I_4N$
FW (g·mol^{-1})	420.70	581.82	659.95	947.33	944.31
Crystal color	colorless	colorless	colorless	colorless	colorless
Cryst. size (mm)	0.25 × 0.23 × 0.20	0.34 × 0.25 × 0.11	0.45 × 0.25 × 0.12	0.31 × 0.30 × 0.14	0.16 × 0.09 × 0.07
Crystal system	trigonal	triclinic	orthorhombic	monoclinic	monoclinic
Space group	$P3_1c$	$P\bar{1}$	$Pnma$	$P2_1/n$	$P2_1/c$
T (K)	293(2)	150(2)	150(2)	150(2)	150(2)
a (Å)	12.3731(3)	4.5919(3)	14.0574(11)	10.0457(2)	10.9075(5)
b (Å)	12.3731(3)	9.1244(6)	7.2070(6)	21.6686(5)	12.2733(5)
c (Å)	9.8020(4)	17.0661(12)	18.6836(14)	12.9568(3)	21.5797(10)
α (°)	90.00	89.153(4)	90.00	90.00	90.00
β (°)	90.00	87.442(3)	90.00	93.892(1)	95.915(2)
γ (°)	120.00	76.337(4)	90.00	90.00	90.00
V (Å^3)	1299.58(7)	694.11(8)	1892.9(3)	2813.88(11)	2873.5(2)
Z	2	2	4	4	4
D_{calc} (g·cm^{-3})	1.075	2.784	2.316	2.236	2.183
μ (mm^{-1})	0.207	6.766	5.087	4.815	4.645
Total refls.	12701	10672	27788	24110	22681
Abs. corr.	multiscan	multiscan	multiscan	multiscan	multiscan
T_{min}, T_{max}	0.662, 0.745	0.143, 0.475	0.237, 0.543	0.245, 0.510	0.612, 0.722
Unique refls.	1983	3082	2344	6401	6517
R_{int}	0.0529	0.0295	0.0458	0.0300	0.0331
Unique refls. ($I > 2\sigma(I)$)	1442	2759	2177	5566	5549
Refined param.	105	163	131	297	280
R_1 ($I > 2\sigma(I)$)	0.0471	0.0210	0.0239	0.0348	0.0574
wR_2 (all data)	0.1259	0.0482	0.0789	0.1047	0.1452
Goodness-of-fit	1.039	1.124	1.213	1.104	1.160
Res. dens (e.Å^{-3})	−0.19, 0.20	−0.51, 0.65	−1.68, 1.58	−1.60, 1.73	−1.60, 2.78

compound	(1)(Et_4N,Br)·S	(1)(Me-DABCO,I)·S	(1)(Bu_3S,I)	(1)(Bu_4N,Br)
Formula	$C_{21}H_{21}Br\ Cl_3F_3I_3N$	$C_{20}H_{16}Cl_3F_3I_4N_2$	$C_{24}H_{27}F_3I_4S$	$C_{28}H_{36}BrF_3I_3N$
FW (g·mol^{-1})	911.35	955.30	912.12	904.19
Crystal color	colorless	colorless	colorless	colorless
Cryst. size (mm)	0.22 × 0.14 × 0.05	0.37 × 0.37 × 0.24	0.23 × 0.12 × 0.05	0.13 × 0.12 × 0.06
Crystal system	monoclinic	monoclinic	monoclinic	monoclinic
Space group	$P2_1/n$	$P2_1/c$	$P2_1/n$	Cc
T (K)	293(2)	293(2)	150(2)	150(2)
a (Å)	9.8382(1)	11.5634(2)	8.6022(2)	14.2433(4)
b (Å)	19.2030(4)	14.1620(3)	26.1613(7)	13.5460(4)
c (Å)	16.0481(3)	17.1705(3)	13.6072(3)	17.5077(4)
α (°)	90.00	90.00	90.00	90.00
β (°)	98.677(1)	97.554(1)	90.273(1)	91.861(2)
γ (°)	90.00	90.00	90.00	90.00
V (Å^3)	2997.15(9)	2787.45(9)	3062.19(13)	3376.15(16)
Z	4	4	4	4
D_{calc} (g·cm^{-3})	2.020	2.276	1.978	1.779
μ (mm^{-1})	4.758	4.791	4.167	3.994
Total refls.	53379	50864	30553	28459
Abs. corr.	multiscan	multiscan	multiscan	multiscan
T_{min}, T_{max}	0.454, 0.788	0.195, 0.317	0.554, 0.812	0.601, 0.787
Unique refls.	6867	6385	7021	7279
R_{int}	0.0642	0.0469	0.0299	0.0600
Unique refls. ($I > 2\sigma(I)$)	4408	4609	6064	5997
Refined param.	289	289	289	325
R_1 ($I > 2\sigma(I)$)	0.0568	0.0374	0.0251	0.0402
wR_2 (all data)	0.1143	0.0954	0.0758	0.0899
Goodness-of-fit	1.077	1.165	1.146	1.058
Res. dens (e.Å^{-3})	−0.83, 1.03	−1.44, 1.15	−0.56, 1.43	−0.85, 0.96

compound	(1)(PPN,Cl)	$(1)_2$(Bu_4N,Br)	$(1)_2$(Ph_3S,Br)	$(1)_2$(Et_3BuN,Br)	$(1)_2$(Et_3S,I)
Formula	$C_{48}H_{30}ClF_3I_3NP_2$	$C_{40}H_{36}BrF_6I_6N$	$C_{42}H_{15}BrF_6I_6S$	$C_{24}BrF_6I_6$[b]	$C_{60}H_{30}F_{12}I_{14}S_2$
FW (g·mol^{-1})	1155.82	1486.01	1506.91	1243.55	2799.40

dx.doi.org/10.1021/ja400740v | J. Am. Chem. Soc. 2013, 135, 6200−6210

Table 4. continued

compound	(**1**)(PPN,Cl)	(**1**)$_2$(Bu$_4$N,Br)	(**1**)$_2$(Ph$_3$S,Br)	(**1**)$_2$(Et$_3$BuN,Br)	(**1**)$_2$(Et$_3$S,I)
Crystal color	colorless	colorless	colorless	colorless	colorless
Cryst. size (mm)	0.26 × 0.11 × 0.05	0.57 × 0.15 × 0.05	0.37 × 0.23 × 0.15	0.35 × 0.20 × 0.11	0.10 × 0.10 × 0.10
Crystal system	triclinic	monoclinic	monoclinic	cubic	cubic
Space group	$P\bar{1}$	$C2/c$	$C2/c$	$Ia\bar{3}$	$Pa\bar{3}$
T (K)	150(2)	293(2)	150(2)	293(2)	150(2)
a (Å)	15.3532(6)	8.88340(10)	11.7331(6)	22.573(5)	22.4310(15)
b (Å)	15.7529(6)	21.3386(4)	15.2250(10)	22.573(5)	22.4310(15)
c (Å)	16.7017(6)	25.8119(5)	25.0661(16)	22.573(5)	22.4310(15)
α (°)	62.9040(10)	90.00	90.00	90.00	90.00
β (°)	62.941(2)	95.6600(10)	97.115(2)	90.00	90.00
γ (°)	61.7050(10)	90.00	90.00	90.00	90.00
V (Å^3)	3015.6(2)	4869.03(14)	4443.2(5)	11502(4)	11286.2(13)
Z	2	4	4	8	4
D_{calc} (g·cm^{-3})	1.273	2.027	2.253	1.436	1.648
μ (mm^{-1})	1.687	4.698	5.196	3.962	3.920
Total refls.	45379	42708	32630	37339	38676
Abs. corr.	multiscan	multiscan	multiscan	multiscan	multiscan
T_{min}, T_{max}	0.800, 0.919	0.434, 0.791	0.248, 0.459	0.402, 0.647	0.676, 0.682
Unique refls.	13586	5518	5054	2207	4318
R_{int}	0.0383	0.0580	0.0409	0.0946	0.0507
Unique refls. ($I > 2\sigma(I)$)	11477	3222	4505	1476	2659
Refined param.	523	245	267	57	144
R_1 ($I > 2\sigma(I)$)	0.0307	0.0491	0.0228	0.0773	0.0644
wR_2 (all data)	0.1030	0.0944	0.0532	0.2193	0.2397
Goodness-of-fit	1.115	1.069	1.084	1.173	1.100
Res. dens (e.Å^{-3})	−0.67, 0.67	−1.31, 1.28	−0.84, 1.16	−0.55, 1.07	−0.82, 1.71

[a] $R_1 = \Sigma||F_o| - |F_c||/\Sigma|F_o|$; $wR_2 = [\Sigma w(F_o^2 - F_c^2)^2/\Sigma wF_o^4]^{1/2}$. [b] The strongly disordered Et_3BuN^+ cation has been squeezed.

anchoring in the structure cavities, while the octahedral coordination is maintained despite a 0.5 occupation parameter for this central iodide atom.

EXPERIMENTAL SECTION

Syntheses. *2,4,6-Tris(trimethylsilylethynyl)-1,3,5-trifluorobenzene.* 2,4,6-Triiodo-1,3,5-trifluorobenzene (2.00 g, 3.9 mmol), $PdCl_2(PPh_3)_2$ (0.275 g, 0.4 mmol), and copper(I) iodide (75 mg, 0.4 mmol) were placed in a dry three necked flask, followed by addition of Et_3N (100 mL). Then, a solution of trimethylsilylacetylene (1.35 g, 13.6 mmol) in Et_3N (50 mL) was added dropwise. At the end of the addition, the mixture was warmed up to 70 °C (oil bath temperature). After 1 h, THF (50 mL) was added, and the mixture was left stirring 16 h under argon. The mixture was filtered over Celite and purified by silica gel column chromatography using hexane as eluant. The product was recrystallized in hexane to afford white needles (0.89 g, 2.1 mmol, 54%): mp 192 °C; ^{1}H NMR ($CDCl_3$, TMS, 300 MHz) δ 0.27 (27H, s, CH_3); ^{19}F NMR ($CDCl_3$, TMS, 300 MHz) δ −99.4 (3F, s); ^{13}C NMR ($CDCl_3$, TMS, 300 MHz) δ 0.0 (CH3), 88.95(d), 107.16 (Ar, q), 161.62 (t), 165.10 (Ar, t). Elem. Anal. Calcd. for $C_{21}H_{27}F_3Si_3$: C, 59.95; H, 6.47%. Found: C, 59.56; H, 6.38%.

2,4,6-Tris(iodoethynyl)-1,3,5-trifluorobenzene. N-Iodosuccinimide (7.52 g, 33.4 mmol) and silver nitrate (2.84 g, 16.7 mmol) were placed in a dry three necked flask, onto which THF (200 mL) and acetone (200 mL) were poured in one portion. Then, 2,4,6-tris(trimethylsilylethynyl)-1,3,5-trifluorobenzene (2.34 g, 5.6 mmol) in solution in THF (200 mL) was added dropwise by dropping funnel, and the mixture was stirred 15 h under argon at room temperature. The mixture was filtered over Celite and purified by silica gel column chromatography using hexane as eluant. The product was recrystallized in a 1/1 mixture of hexane/dichloromethane to afford white needles (1.90 g, 3.3 mmol, 59%): mp > 180 °C (decomp.); ^{19}F NMR ($CDCl_3$, TMS, 300 MHz) δ −99.4 (3F, s); ^{13}C NMR ($CDCl_3$, TMS, 300 MHz) δ 19.50, 78.21, 162.90, 166.39. Elem. Anal. Calcd. for C: 24.77%. Found: 24.60%

Ternary Salts Preparation. All ternary salts were obtained from slow evaporation of solutions of the desired salt in $CHCl_3$ (1.5−2.0 mL) and **1** in $CHCl_3$ (1.5−2.0 mL), as detailed in Table 3. Colorless crystals were isolated in every case and used directly for X-ray diffraction, as they often lose easily included solvent molecules.

Crystallography. For low temperature X-ray data collections, single crystals were taken in a loop in oil and put directly under the N_2 stream at 150 K to avoid solvent losses. Data were collected on a Bruker SMART II diffractometer with graphite-monochromated Mo−Kα radiation (λ = 0.71073 Å). For room temperature X-ray data collections, crystals were glued on the top of a thin glass fiber. X-ray data were collected on a Nonius KappaCCD with graphite-monochromated Mo−Kα radiation (λ = 0.71073 Å). All structures were solved by direct methods (SHELXS-97, SIR97)[40] and refined (SHELXL-97) by full-matrix least-squares methods,[41] as implemented in the WinGX software package.[42] Absorption corrections were applied. Hydrogen atoms were introduced at calculated positions (riding model), included in structure factor calculations, and not refined. A SQUEEZE procedure was applied to the structure of (**1**)$_2$(Et_3BuN,Br), where the whole Et_3BuN^+ cation could not be properly localized (see text). Voids in the two cubic structures (Figures 12 and 14) were represented using Mercury (Voids, Contact Surface).[43] Crystallographic data are summarized in Table 4.

ASSOCIATED CONTENT

Supporting Information

CIF file for the 14 X-ray crystal structures. This material is available free of charge via the Internet at http://pubs.acs.org.

AUTHOR INFORMATION

Corresponding Author

marc.fourmigue@univ-rennes1.fr

Notes

The authors declare no competing financial interest.

■ ACKNOWLEDGMENTS

This work was performed with the financial support of the ANR (Paris, France) under contract no. ANR-08-BLANC-0091-02. We also thank the CDIFX (Rennes, France) for access to diffractometer facilities.

■ REFERENCES

(1) (a) Special issue: 35 Years of Synthetic Anion Receptor Chemistry 1968−2003. Gale, P. A. *Coord. Chem. Rev.* **2003**, *240*, 1−226. (b) Special issue: Anion Coordination Chemistry II. Gale, P. A. *Coord. Chem. Rev.* **2006**, *250*, 2917−3244.

(2) (a) Park, C. H.; Simmons, H. E. *J. Am. Chem. Soc.* **1968**, *90*, 2431. (b) Graf, E.; Lehn, J.-M. *J. Am. Chem. Soc.* **1976**, *98*, 6403. (c) Schmidtchen, F. P. *Angew. Chem., Int. Ed. Engl.* **1977**, *16*, 720. (d) Schmidtchen, F. P.; Muller, G. *J. Chem. Soc., Chem. Commun.* **1984**, 1115.

(3) (a) Yang, X.; Knobler, C. B.; Hawthorne, M. F. *Angew. Chem., Int. Ed. Engl.* **1991**, *30*, 1507. (b) Azuma, Y.; Newcomb, M. *Organometallics* **1984**, *3*, 9. (c) Katz, H. E. *Organometallics* **1987**, *6*, 1134. (d) Tamao, K.; Hayashi, T.; Ito, Y. *J. Organomet. Chem.* **1996**, *506*, 85.

(4) Gamez, P.; Mooibroek, T. J.; Teat, S. J.; Reedijk, J. *Acc. Chem. Res.* **2007**, *40*, 435.

(5) (a) Legon, A. C. *Angew. Chem., Int. Ed.* **1999**, *38*, 2687. (b) Desiraju, G. R.; Harlow, R. L. *J. Am. Chem. Soc.* **1989**, *111*, 6757.

(6) (a) Metrangolo, P.; Pilati, T.; Terraneo, G.; Biella, S.; Resnati, G. *CrystEngComm* **2009**, *11*, 1187. (b) Cavallo, G.; Metrangolo, P.; Pilati, T.; Resnati, G.; Sansoterra, M.; Terraneo, G. *Chem. Soc. Rev.* **2010**, *39*, 3772.

(7) (a) Caballero, A.; Zapata, F.; White, N. G.; Costa, P. J.; Félix, V.; Beer, P. D. *Angew. Chem., Int. Ed.* **2012**, *51*, 1876. (b) Caballero, A.; White, N. G.; Beer, P. D. *Angew. Chem., Int. Ed.* **2011**, *50*, 1845. (c) Casnati, A.; Cavallo, G.; Metrangolo, P.; Resnati, G.; Ugozzoli, F.; Ungaro, R. *Chem.—Eur. J.* **2009**, *15*, 7903.

(8) (a) Clark, T.; Hennemann, M.; Murray, J. S.; Politzer, P. *J. Mol. Model.* **2007**, *13*, 291. (b) Politzer, P.; Murray, J. S.; Concha, M. C. *J. Mol. Model.* **2007**, *13*, 643. (c) Murray, J. S.; Lane, P.; Politzer, P. *Int. J. Quantum Chem.* **2007**, *107*, 2286. (d) Politzer, P.; Murray, J. S.; Lane, P. *Int. J. Quantum Chem.* **2007**, *107*, 3046. (e) Mohajeri, A.; Pakiari, A. H.; Bagheri, N. *Chem. Phys. Lett.* **2009**, *467*, 393.

(9) Tsuzuki, S.; Wakisaka, A.; Ono, T.; Sonoda, T. *Chem.—Eur. J.* **2012**, *18*, 951.

(10) (a) Farina, A.; Meille, V. S.; Messina, M. T.; Metrangolo, P.; Resnati, G. *Angew. Chem., Int. Ed.* **1999**, *38*, 2433. (b) Messina, M. T.; Metrangolo, P.; Panzeri, W.; Pilati, T.; Resnati, G. *Tetrahedron* **2001**, *57*, 8543.

(11) (a) Weiss, R.; Rechinger, M.; Hampel, F.; Wolski, A. *Angew. Chem., Int. Ed. Engl.* **1995**, *34*, 441. (b) Ghassemzadeh, M.; Harms, K.; Dehnicke, K. *Chem. Ber.* **1996**, *129*, 115. (c) Ghassemzadeh, M.; Harms, K.; Dehnicke, K. *Chem. Ber.* **1996**, *129*, 259. (d) Ghassemzadeh, M.; Harms, K.; Dehnicke, K. *Z. Naturforsch.* **1997**, *B52*, 772. (e) Ghassemzadeh, M.; Magull, J.; Fenske, D.; Dehnicke, K. *Z. Naturforsch.* **1996**, *B51*, 1579.

(12) (a) Dunitz, J. D.; Gehrer, H.; Britton, D. *Acta Crystallogr.* **1972**, *28*, 1989. (b) Yamamoto, H. M.; Yamaura, J.-I.; Kato, R. *J. Mater. Chem.* **1998**, *8*, 15.

(13) (a) Grebe, J.; Geiseler, G.; Harms, K.; Dehnicke, K. *Z. Naturforsch.* **1999**, *B54*, 77. (b) Abate, A.; Biella, S.; Cavallo, G.; Meyer, F.; Neukirch, H.; Metrangolo, P.; Pilati, T.; Resnati, G.; Terraneo, G. *J. Fluorine Chem.* **2009**, *130*, 1171.

(14) (a) Yamamoto, H. M.; Maeda, R.; Yamaura, J.-I.; Kato, R. *J. Mater. Chem.* **2001**, *11*, 1034. (b) Barres, A.-L.; El-Ghayoury, A.; Zorina, L . V.; Canadell, E.; Auban-Senzier, P.; Batail, P. *Chem. Commun.* **2008**, 2194.

(15) Bock, H.; Holl, S. *Z. Naturforsch.* **2002**, *B57*, 713.

(16) Lindeman, S. V.; Hecht, J.; Kochi, J. K. *J. Am. Chem. Soc.* **2003**, *125*, 11597.

(17) (a) Yaghi, O. M.; Li, H.; Davis, C.; Richardson, D.; Groy, T. L. *Acc. Chem. Res.* **1998**, *31*, 474. (b) Batten, S. R. *Curr. Opin. Solid State Mater. Sci.* **2001**, *5*, 107. (c) Moulton, B.; Zaworotko, M. J. *Chem. Rev.* **2001**, *101*, 1629. (d) Janiak, C. *Dalton Trans.* **2003**, 2781. (e) Kitagawa, S.; Kitaura, R.; Noro, S. *Angew. Chem., Int. Ed.* **2004**, *43*, 2334. (f) Rosseinsky, M. J. *Microporous Mesoporous Mater.* **2004**, *73*, 15.

(18) Cook, T. R.; Zheng, Y.-R.; Stang, P. J. *Chem. Rev.* **2013**, *113*, 734.

(19) (a) Yamamoto, H. M.; Yamaura, J.-I.; Kato, R. *J. Am. Chem. Soc* **1998**, *120*, 5905. (b) Yamamoto, H. M.; Yamaura, J.-I.; Kato, R. *Synth. Met.* **1999**, *102*, 1448. (c) Yamamoto, H. M.; Kato, R. *Chem. Lett.* **2000**, 970. (d) Kosaka, Y.; Yamamoto, H. M.; Nakao, A.; Kato, R. *Bull. Chem. Soc. Jpn.* **2006**, *79*, 1148.

(20) Yamamoto, H. M.; Kosaka, Y.; Maeda, R.; Yamaura, J.-I.; Nakao, A.; Nakamura, T.; Kato, R. *ACS Nano* **2008**, *2*, 143.

(21) Lieffrig, J.; Yamamoto, H. M.; Kusamoto, T.; Cui, H.; Fourmigué, M.; Kato, R. *Cryst. Growth Des.* **2011**, *11*, 4267.

(22) Metrangolo, P.; Meyer, F.; Pilati, T.; Resnati, G.; Terraneo, G. *Chem. Commun.* **2008**, 1635.

(23) Triguero, S.; Llusar, R.; Polo, V.; Fourmigué, M. *Cryst. Growth Des.* **2008**, *8*, 2241.

(24) Nishikawa, T.; Shibuya, S.; Hosokawa, S.; Isobe, M. *Synlett* **1994**, 485.

(25) Eccles, K. S.; Morrison, R. E.; Stokes, S. P.; O'Mahony, G. E.; Hayes, J. A.; Kelly, D. M.; O'Boyle, N. M.; Fábián, L.; Moynihan, H. A.; Maguire, A. R.; Lawrence, S. E. *Cryst. Growth Des.* **2012**, *12*, 2969.

(26) (a) Liantonio, R.; Metrangolo, P.; Meyer, F.; Pilati, T.; Navarrini, W.; Resnati, G. *Chem. Commun.* **2006**, 1819. (b) Metrangolo, P.; Meyer, F.; Pilati, T.; Proserpio, D. M.; Resnati, G. *Chem.—Eur. J.* **2007**, *13*, 5765.

(27) Thaimattam, R.; Sharma, C. V. K.; Clearfield, A.; Desiraju, G. R. *Cryst. Growth. Des.* **2001**, *1*, 103.

(28) Blatov, V. A.; Carlucci, L.; Ciani, G.; Proserpio, D. M. *CrystEngComm.* **2004**, *6*, 377.

(29) Chae, H. K.; Kim, J.; Friedrichs, O. D.; O'Keeffe, M.; Yaghi, O. M. *Angew. Chem., Int. Ed.* **2003**, *42*, 3907.

(30) O'Keeffe, M.; Eddaoudi, M.; Li, H.; Reineke, M.; Yaghi, O. M. *J. Solid State Chem.* **2000**, *152*, 3.

(31) (a) Batten, S. R.; Robson, R. *Angew. Chem., Int. Ed.* **1998**, *37*, 1460. (b) Kroll, P.; Riedel, R.; Hoffmann, R. *Phys. Rev. B* **1999**, *60*, 3126. (c) Miller, J. S. *Adv. Mater.* **2001**, *13*, 525. (d) Batten, S. R.; Hoskins, B. F.; Moubaraki, B.; Murray, K. S.; Robson, R. *J. Chem. Soc., Dalton Trans.* **1999**, 2977.

(32) (a) Tzeng, B.-C.; Chiu, T.-H.; Chen, B.-S.; Lee, G.-H. *Chem.—Eur. J.* **2008**, *14*, 5237. (b) Hasegawa, S.; Horike, S.; Matsuda, R.; Furukawa, S.; Mochizuki, K.; Kinoshita, Y.; Kitagawa, S. *J. Am. Chem. Soc.* **2007**, *129*, 2607.

(33) (a) Stevens, E. D.; de Lucia, M. L.; Coppens, P. *Inorg. Chem.* **1980**, *19*, 813. (b) Bayliss, P. *Am. Mineral.* **1977**, *62*, 1168.

(34) Laughlin, R. G. *The Aqueous Phase Behaviour of Surfactants*; Academic Press: London (UK), 1994.

(35) Imperor-Clerc, M. *Curr. Opin. Colloid Interface Sci.* **2005**, *9*, 370.

(36) Clerc, M.; Levelut, A.-M.; Sadoc, J.-F. *J. Phys. II* **1991**, *1*, 1263.

(37) Forster, S.; Khandpur, A. K.; Zhao, J.; Bates, F. S.; Hamley, I. W.; Ryan, A. J.; Bras, W. *Macromolecules* **1994**, *27*, 6922.

(38) Landry, C. C.; Tolbert, S. H.; Gallis, K. W.; Monnier, A.; Stucky, G. D.; Norby, F.; Hanson, J. C. *Chem. Mater.* **2001**, *13*, 1600.

(39) (a) Ward, M. D.; Horner, M. J. *CrystEngComm* **2004**, *6*, 401. (b) Horner, M. J.; Holman, K. T.; Ward, M. D. *J. Am. Chem. Soc.* **2007**, *129*, 14640.

(40) Altomare, A.; Burla, M. C.; Camalli, M.; Cascarano, G.; Giacovazzo, C.; Guagliardi, A.; Moliterni, A. G. G.; Polidori, G.; Spagna, R. *J. Appl. Crystallogr.* **1999**, *32*, 115.

(41) Sheldrick, G. M. *SHELX97—Programs for Crystal Structure Analysis*, Bruker AXS: Madison WI, Release 97−2; 1998.

(42) Farrugia, L. J. *J. Appl. Crystallogr.* **1999**, *32*, 837.

(43) Barbour, L. J. *Chem. Commun.* **2006**, 1163.